First-principles study of the thermodynamics of hydrogen-vacancy interaction in fcc iron

R. Nazarov,* T. Hickel, and J. Neugebauer
Max-Planck Institut für Eisenforschung GmbH, D-40237 Düsseldorf, Germany
(Received 31 August 2010; published 9 December 2010)

The interaction of vacancies and hydrogen in an fcc iron bulk crystal was studied combining thermodynamic concepts with *ab initio* calculations and considering various magnetic structures. We show that up to six H atoms can be trapped by a monovacancy. All of the studied point defects (single vacancy, H in interstitial positions, and H-vacancy complexes) cause an anisotropic elastic field in antiferromagnetic fcc iron and significantly change the local and total magnetization of the system. The proposed thermodynamical model allows the determination of the equilibrium vacancy concentration and the concentration of dissolved hydrogen for a given temperature and H chemical potential in the reservoir. For H-rich conditions a dramatic increase in the vacancy concentration in the crystal is found.

DOI: 10.1103/PhysRevB.82.224104 PACS number(s): 61.72.J−, 05.70.−a, 81.05.Bx, 62.20.mm

I. INTRODUCTION

Hydrogen embrittlement of metals is one of the most fundamental problems in modern materials physics and directly relevant to the large number of structural materials that are adversely affected by hydrogen,[1,2] including novel high-strength steels and aluminum alloys. Despite being under investigation already for centuries, a full understanding of the responsible mechanisms in many metals is still lacking. In particular the underlying physics of hydrogen embrittlement is not known in modern high-strength austenitic steels, where the fcc structure of Fe is, e.g., stabilized by the addition of Mn. Several mechanisms of hydrogen embrittlement have been proposed in the past:[1,3] (1) hydrogen-enhanced decohesion, (2) formation of other, usually brittle phases (hydrides, martensite in steels), (3) hydrogen-enhanced localized plasticity, and (4) hydrogen trapping in voids (bubbles, blisters). None of these mechanisms alone can explain the complex physics related to hydrogen embrittlement in various material systems. Instead, a combination of them is supposed to be responsible for hydrogen degradation of metals.

The activation of each of these mechanisms is related to the interaction of dissolved H with defects of the crystal structure. The concept of hydrogen-enhanced localized plasticity, for example, assumes that H in the vicinity of a dislocation reduces the energetic barrier for dislocation motion, thus increasing its mobility and locally decreasing the yield stress.[4]

The interaction of H with vacancies could potentially be the reason for several hydrogen-related processes since vacancies serve as trapping centers for dissolved H and can locally yield a critical H concentration sufficient for initiating several mechanisms of hydrogen embrittlement. Previous *ab initio* calculations revealed that up to 12 H atoms can be trapped by a monovacancy in Al,[5] up to 6 in Pd,[6] up to 5 in bcc Fe.[7] The formation energy of such vacancy-hydrogen complexes is lower than the sum of the energies for incorporating a pure vacancy and isolated interstitial H atoms into the bulk material. Therefore, the formation of H-vacancy complexes simultaneously increases both the concentration of vacancies *and* the total hydrogen content in the metal. That such a phenomenon can have a very significant effect, becomes apparent, e.g., in the case of Pd, where it leads to the formation of up to 23% of vacancies in a hydrogen-rich atmosphere.[8] These high concentrations even result in the formation of vacancy-ordered structures.[9,10] After its first discovery in Pd (Refs. 11–13) and also in Ni (Refs. 14 and 15) this effect is now known in many more material systems such as in Ti,[16] Pd-Rh alloys,[17] Al,[18] Mn,[19] Fe,[19,20] Cr,[21] and Co.[19] The special case of supercritical vacancy concentration is generally referred to as superabundant vacancy (SAV) formation.

A reliable theoretical simulation of SAV formation can be achieved when combining thermodynamic principles with *ab initio* results for formation energies of vacancies, vacancy-solute complexes and solution enthalpies of hydrogen in bulk metals. Such an approach was proposed previously, e.g., by Monasterio *et al.*[22] for the interaction between vacancies and solute hydrogen and carbon in bcc Fe. In their model, *ab initio* formation energies of different point-defect clusters were used for a minimization of a free energy functional. The total concentration of vacancies and of carbon and hydrogen atoms was kept constant during the simulation. Whereas this assumption yields a reliable description at low temperatures, where diffusion prevents equilibration, a thermodynamically open model is needed for higher temperatures. Only in this way can the dependence on hydrogen chemical potentials, the high diffusivity of H, and the accelerated self-diffusion of Fe (and vacancies formation) at sufficiently high temperatures be considered. The work of Gavriljuk *et al.*[23] is an important step in this direction since it considers a temperature-dependent concentration of equilibrium vacancies based on a mean-field approximation.[24,25] The total amount of hydrogen in the Fe crystal however is assumed to be constant. Maroevic and McLellan[26] used Dirac statistics to describe the distribution of hydrogen-vacancy complexes. Their simulations were based on experimental information for formation energies.[14] However, the agreement with experiment was unsatisfactory.[13] A semiempirical model of vacancy concentration was also proposed by Fukai[27] based on Maxwell-Boltzmann statistics, which is expected to be a reliable approach at small concentration. Similar to the previous work, experimental input parameters and only an average number of H atoms trapped by vacancies were considered. Using this scheme, a much better agreement with

experiment could be achieved. A very promising approach has been recently suggested by Ji *et al.*[28] They have described SAV formation in Al using a grand canonical ensemble, and treating the chemical potentials of each component and the numbers of different point defects as variables. Despite the finding of Lu *et al.*[5] that up to 12 H atoms can be trapped by a monovacancy in Al, the complexity of the approach restricted Ji *et al.*[28] to H-vacancy complexes with a maximum occupation of 2 H atoms.

A further challenge in describing this system is that an *ab initio* description of defect formation in γ-Fe is complicated by the magnetic properties of this phase. Previous density-functional-theory (DFT) calculations with collinear spin orientations[29] found the ground state of γ-Fe to be an antiferromagnetic double layer (AFMD) structure. A transition to a ferromagnetic (FM) high-spin state at volumes above the equilibrium value and to another antiferromagnetic structure at high pressures is reported. Recent DFT calculations[30] even showed that the ground state of γ-Fe is a spin-spiral state having a wave vector varying with atomic volume. However, the energy difference to the AFMD order is only a few meV/atom at 0K. Further, the lattice constant between these two structures differs by only 0.01 Å. Therefore, the AFMD structure can be considered as a good representative of the magnetic ground state of γ-Fe. A direct comparison of the obtained theoretical predictions with experiments is difficult, since the fcc phase of pure Fe exists only at high temperatures (between 1185 and 1667 K), unless it is artificially stabilized, e.g., in the form of nanosized precipitates in bulk fcc Cu,[31] as ultrathin films on Cu(100) or Cu(111) substrates[32–34] and more recently on Ir(100) substrates.[35] Nevertheless, the fcc phase is of utmost importance in modern austenitic steels, where the stabilization is due to the presence of alloying elements such as Mn, Ni, and C. In many cases, the effect of these alloying elements on the magnetization is unknown.

An accurate description of point defects in such complex magnetic structures is challenging. State-of-the-art *ab initio* calculations of defect structures in Fe include the carbon impurity in the octahedral site in AFMD fcc Fe (Ref. 36) whereas *ab initio* results for vacancies in Fe are known for the FM bcc phase.[37] In the present study we have performed defect calculations (in particular, vacancies, interstitial H, and H-vacancy complexes) in fcc Fe. To estimate the importance of magnetism a collinear AFMD structure as well as nonmagnetic (NM) fcc Fe are considered. The calculated formation energies of different defects are then used to obtain equilibrium concentrations of hydrogen, Fe vacancies, and their complexes in γ-Fe.

The paper is organized as follows: in Sec. II we present the technical aspects of the *ab initio* calculations and introduce our thermodynamic model. In Sec. III we discuss the DFT results on the monovacancies, single hydrogen impurities, and vacancy-hydrogen complexes. Particular attention is paid in this section to the influence of a vacancy or H atoms on the magnetic moments of the host Fe atoms. Based on our thermodynamic model we present in the next section equilibrium concentrations and solubility limits of H, vacancies and their complexes in fcc Fe. Conclusions are given in Sec. V.

II. METHODOLOGY

A. DFT calculations

The energetics and equilibrium structure of the defects have been calculated employing DFT (Refs. 38 and 39) calculations within the generalized gradient approximation of the Perdew-Burke-Ernzerhof (PBE) form[40] for electron exchange and correlation, using the Vienna *Ab Initio* Simulation Package.[41–43] Our convergence tests showed that a kinetic energy cutoff of 300 eV and a 6912 k-points·atoms mesh are sufficient to achieve an accuracy in the electronic energy below 2 meV/atom. Structural relaxations were performed until the forces on each atom were below 0.01 eV/Å.

The first-order Methfessel-Paxton method[44] is used for the Fermi-surface smearing in order to obtain accurate forces, and a smearing width of 0.1 eV is chosen such that the error in the 0 K extrapolated energy is less than 1 meV/atom. Both cell-shape and atomic positions are fully relaxed in all calculations, unless specified otherwise.

Using these parameters, we obtain for the fcc Fe lattice constant a value of 3.45 Å in the nonmagnetic state and of $a=3.46$ Å, $c=3.74$ Å in the antiferromagnetic double-layer state, where the magnitude of the local magnetic moment of each atom is 2.05 μ_B (μ_B is the Bohr magneton). The results are in good agreement with previous DFT-generalized gradient approximation (GGA) calculations.[30]

Point defects in the crystal structure induce local relaxations and may thus change the bulk lattice constant. For sufficiently high defect concentrations this effect becomes sizeable and can be used, e.g., to measure defect concentrations using standard x-ray techniques. In order to relate the change in the crystal lattice constant to the defect concentration, we determine the defect formation volume

$$\Omega_f^{\mathrm{def}} = N_{\mathrm{sites}}\Omega - (N_{\mathrm{sites}} - \Delta n_{\mathrm{Fe}})\Omega_0. \quad (1)$$

Here, N_{sites} is the number of lattice sites in the supercell, Ω is the volume per site in the supercell with a defect, Ω_0 is the atomic volume in the undisturbed bulk material, and Δn_{Fe} is the change in the number of Fe atoms in the supercell due to the presence of a defect.

The equilibrium concentration of defects is thermodynamically related to their formation energies

$$E_f^{\mathrm{def}} = \epsilon^{\mathrm{def}} - \mu_{\mathrm{Fe}}^0 \Delta n_{\mathrm{Fe}} - \mu_{\mathrm{H}}^0 \Delta n_{\mathrm{H}}, \quad (2)$$

$$\epsilon^{\mathrm{def}} = E_{\mathrm{tot}}^{\mathrm{def}} - E_{\mathrm{tot}}^{\mathrm{bulk}}, \quad (3)$$

where $E_{\mathrm{tot}}^{\mathrm{def}}$ and $E_{\mathrm{tot}}^{\mathrm{bulk}}$ are the total energies of the considered fcc Fe supercells, respectively, with and without a defect, μ_X^0 is the chemical potential of X and Δn_{H} is the change in the number of H atoms in these two supercells. A pure bulk fcc Fe structure has been taken as the reference for the chemical potential of Fe ($\mu_{\mathrm{Fe}}^0 = E_{\mathrm{tot}}^{\mathrm{bulk}}/n_{\mathrm{Fe}}$, where n_{Fe} is the number of Fe atoms in the bulk reference cell). The H_2 molecule, simulated in a cubic box with 10 Å length, was taken as the reference for the chemical potential of hydrogen. We obtained for H_2 a bond length of 0.75 Å, and a binding energy of 4.47 eV, almost identical to previous GGA results[45] and in

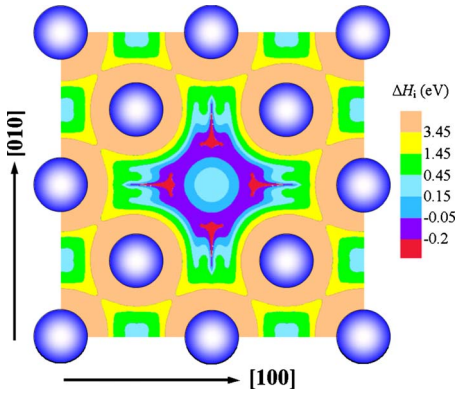

FIG. 1. (Color online) Potential energy surface of interstitial H in the (001) plane in nonmagnetic fcc Fe. The vacancy is in the center. The energetically preferred places for H are situated in the ⟨100⟩ directions from the vacancy center. The local minima in the bulk like regions correspond to the octahedral site.

fair agreement with experimental values[46] of 0.74 Å and 4.75 eV.

To identify the most preferable positions for H within and around a vacancy we have mapped the full three-dimensional potential energy surface of interstitial H (see Fig. 1). For the calculation of this energy surface the host Fe atoms (except corner atoms of the supercell to prevent a motion or rotation of the structure) have been allowed to relax. The potential energy surface reveals three inequivalent local minima corresponding to (meta) stable sites that can be occupied by H: the tetrahedral (TS) and octahedral sites (OS) and vacancies. As also shown in Fig. 1, there are several pronounced energetic minima within a single vacancy.

The tendency to add/remove an H atom to an existing vacancy-hydrogen complex is determined by a positive/negative reaction enthalpy

$$\Delta H_i = E_{\mathrm{f}}^{i\text{H-vac}} - E_{\mathrm{f}}^{(i-1)\text{H-vac}} - \mu_{\mathrm{H}}^0, \tag{4}$$

where $E_{\mathrm{f}}^{i\text{H-vac}}$ and $E_{\mathrm{f}}^{(i-1)\text{H-vac}}$ are the formation energies of hydrogen-vacancy complexes with i and $i-1$ H atoms, respectively.

The formation energy of defects in fcc Fe is strongly influenced by the magnetic structure and the magnitude of the magnetic moments in their neighborhood. Since our calculations also show that vacancies modify the surrounding magnetic structure we have performed a systematic search to identify the stable ones for each magnetic configuration. The search was performed by using random initial magnetizations for all nonequivalent atoms in the considered supercell [see Fig. 2(a)]. Repeating this procedure several times, we obtained the identical magnetic structure that is also lowest in energy (in more than 90% of the calculations). The local magnetic moments found for the H-free vacancy were used as initial guesses for the magnetic moments when calculating the H-vacancy complexes.

The local magnetic moments of all symmetry inequivalent Fe atoms were obtained from a Bader analysis.[47,48] This analysis uses as sole input the charge density and considers the zero-flux surfaces as the borders between different atoms.

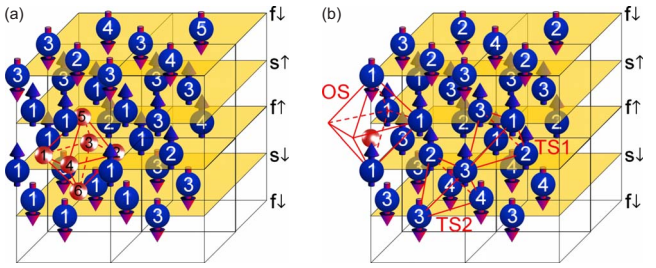

FIG. 2. (Color online) Different atomic shells around (a) a vacancy and (b) an H atom in an octahedral site in an AFMD magnetic structure. The supercell is a $2\times2\times2$ repetition of the conventional fcc unit cell. The labeling of planes includes the differentiation between the first and the second plane with the same spin direction, and the direction of the individual spins. Possible positions of H in a vacancy are shown by the red (lightest) balls. The position of H in octahedral interstitial site (marked by dashed octahedron) is displaced from its center. Two variants of tetrahedral sites are marked by dashed tetrahedrons.

Using these borders to define the volume related to each atom, the local magnetization and charge of each atom are obtained by integrating the spin density over this volume.

B. Thermodynamic model

In thermodynamic equilibrium the vacancy concentration in an H-containing Fe crystal is determined by the temperature as well as the hydrogen chemical potential. In order to express this correspondence analytically, we start from the model proposed by Ji *et al.*[28] and extend the original formulation that was restricted to an occupancy of two to an arbitrary number of H atoms in a vacancy. To derive our model, we consider a vacancy-containing crystal, which is in thermodynamic equilibrium with a hydrogen reservoir. All relevant point defects are considered including empty vacancies, vacancies with a certain number of incorporated hydrogen atoms and hydrogen atoms in interstitial (i.e., octahedral and tetrahedral) sites. Complexes consisting of several vacancies turned out to be energetically not relevant.

Assuming that H is able to freely move in and out of the bulk system in the relevant time scales, the system is thermodynamically open and we use the grand canonical potential

$$J = U - TS + pV - N_{\mathrm{Fe}}\mu_{\mathrm{Fe}} - N_{\mathrm{H}}\mu_{\mathrm{H}}. \tag{5}$$

Here U, S, and V are extensive parameters representing the internal energy, the entropy, and the volume of the crystal, and T and p are intensive parameters representing the temperature and the pressure in the system. The Fe chemical potential μ_{Fe} is determined by the equilibrium with fcc Fe bulk and its temperature and pressure dependence is negligible on the energy scale relevant for defect formation, i.e., $\mu_{\mathrm{Fe}}=\mu_{\mathrm{Fe}}^0$. This is not the case for the H chemical potential μ_{H}, which is determined by the reservoir (atmosphere, electrolyte) in which the Fe crystal is embedded.

Equation (5) incorporates via N_{Fe} and N_{H} the numbers of Fe and H atoms in the crystal, which depend on the defects in the crystal. Each of the point-defect complexes considered

in this work (labeled with index "i") is characterized by the number of involved vacancies n_i^{vac} (in this work limited to $n_i^{\mathrm{vac}}=0$ or 1), the number of involved hydrogen atoms n_i^{H} (the total number of distinguishable configurations for a single cluster is N_i^{conf}) and the number of occurrences N_i of the specific defect complex i in the crystal. Based on these definitions the following equations hold:

$$N_{\mathrm{H}} = \sum_i n_i^{\mathrm{H}} N_i, \tag{6}$$

$$N_{\mathrm{vac}} = \sum_i n_i^{\mathrm{vac}} N_i, \tag{7}$$

$$N_{\mathrm{Fe}} = N_{\mathrm{sites}} - N_{\mathrm{vac}}. \tag{8}$$

Considering a defect-free crystal as reference and neglecting vibrational contributions, the internal energy in Eq. (5) is directly related to the presence of these defects

$$U = \sum_i N_i \epsilon_i, \tag{9}$$

each of which has an energy ϵ_i defined by Eq. (3). We apply here the independent point defect approximation, which implies that the formation energies of different point defects are independent of their concentrations.

The configurational entropy can be written in the following way:

$$S = k_B \ln(W_{\mathrm{vac}} W_{\mathrm{H}}^{\mathrm{int}} W_{\mathrm{H}}^{\mathrm{vac}}). \tag{10}$$

Here W_{vac} denotes the number of configurations related to the removal of host Fe atoms and the creation of vacancies (or H-vacancy complexes), $W_{\mathrm{H}}^{\mathrm{int}}$ represents the configuration space for the distribution of H in interstitial sites, $W_{\mathrm{H}}^{\mathrm{vac}}$ gives the number of configurations of H within H-vacancy complexes.

The number of ways to distribute N_{vac} vacancies over the N_{sites} host sites is

$$W_{\mathrm{vac}} = \frac{N_{\mathrm{sites}}!}{(N_{\mathrm{sites}} - N_{\mathrm{vac}})!} \prod_i^{\{n_i^{\mathrm{vac}}=1\}} \frac{1}{N_i!}, \tag{11}$$

where the upper bound on the product indicates that only defects i which involve a vacancy ($n_i^{\mathrm{vac}}=1$) are considered here. The numerator of Eq. (11) is the number of possible sites on which vacancies can be distributed and the denominator accounts for the fact that all nonvacancy sites as well as all vacancies of the same type are identical. The generalized expression for the number of configurations of H-vacancy complexes is

$$W_{\mathrm{H}}^{\mathrm{vac}} = \prod_i^{\{n_i^{\mathrm{vac}}=1\}} (N_i^{\mathrm{conf}})^{N_i}. \tag{12}$$

The configurational space for a H distribution in interstitial positions (defects with the constraint $n_i^{\mathrm{vac}}=0$) is determined by

$$W_{\mathrm{H}}^{\mathrm{int}} = \prod_i^{\{n_i^{\mathrm{vac}}=0\}} \frac{N_i^{\mathrm{int}}!}{(N_i^{\mathrm{int}} - N_i)! N_i!}, \tag{13}$$

where in the numerator the total number $N_i^{\mathrm{int}} = z_i^{\mathrm{sites}} N_{\mathrm{sites}} - z_i^{\mathrm{vac}} N_{\mathrm{vac}}$ of interstitial sites appears, taking their reduction due to the presence of vacancies into account. z_i^{sites} gives the ratio between interstitial sites and lattice sites in bulk whereas z_i^{vac} represents the number of interstitial sites of type i removed by a single vacancy. The denominator takes into account that all distributed H atoms in the specific interstitial sites i are identical and all nonoccupied interstitial sites of the same type are also identical.

Assuming constant pressure, the volume of the crystal varies with the number of included defects as

$$V = \sum_i N_i (\Omega_{\mathrm{f}}^i - \Omega^0). \tag{14}$$

Here Ω_{f}^i is the formation volume of a defect i defined by Eq. (1). The formation enthalpy of hydrogen-containing defects is a function of the H chemical potential

$$H_{\mathrm{f}}^i = \epsilon_i + p(\Omega_{\mathrm{f}}^i - \Omega^0) - n_i^{\mathrm{vac}} \mu_{\mathrm{Fe}}^0 + n_i^{\mathrm{H}} \mu_{\mathrm{H}}. \tag{15}$$

In thermodynamic equilibrium the grand canonical potential of the system is minimal with respect to the number of any point defect or complex i

$$\frac{\partial J}{\partial N_i} = 0. \tag{16}$$

After straightforward transformations we obtain a set of equations for all interstitials ($n_i^{\mathrm{vac}}=0$)

$$N_i = \frac{N_i^{\mathrm{int}}}{1 + \exp\left(\frac{H_{\mathrm{f}}^i}{k_B T}\right)} \tag{17}$$

and a coupled set of equations for all H-vacancy complexes ($n_i^{\mathrm{vac}}=1$)

$$N_i = N_i^{\mathrm{conf}} (N_{\mathrm{sites}} - N_{\mathrm{vac}}) C \exp\left(-\frac{H_{\mathrm{f}}^i}{k_B T}\right). \tag{18}$$

The latter contains a correction term

$$C = \prod_i^{\{n_i^{\mathrm{vac}}=0\}} \left(1 - \frac{N_i}{N_i^{\mathrm{int}}}\right)^{z_i^{\mathrm{vac}}}, \tag{19}$$

$$= \prod_i^{\{n_i^{\mathrm{vac}}=0\}} \left(1 + \exp\left(-\frac{H_{\mathrm{f}}^i}{k_B T}\right)\right)^{-z_i^{\mathrm{vac}}}, \tag{20}$$

which takes into account that a vacancy can only be formed if all z_i^{vac} involved interstitial sites of type i are not already occupied by a H atom. The probability of such an occupation is given by the fraction $\frac{N_i}{N_i^{\mathrm{int}}}$, including self-consistently the number of vacancies N_{vac} as part of N_i^{int}.

By inserting Eq. (18) into Eq. (7) we get an analytical solution for the total vacancy concentration

$$N_{\mathrm{vac}} = \frac{N_{\mathrm{sites}}}{1 + \left[C \sum_i n_i^{\mathrm{vac}} N_i^{\mathrm{conf}} \exp\left(- \frac{H_{\mathrm{f}}^i}{k_B T} \right) \right]^{-1}}. \quad (21)$$

The above equations are general and allow, by application of well-defined approximations, the derivation of all previously applied/proposed formalisms. Neglecting that the creation of vacancies removes bulk interstitial sites (i.e., assuming $z_i^{\mathrm{vac}}=0$) results in a Fermi-Dirac statistics as used by Monasterio *et al.*[22] In the low-concentration limit ($H_{\mathrm{f}}^i \gg k_B T$) the Fermi-Dirac statistics approaches Boltzmann statistics[49] with a prefactor equal to the number of energetically degenerate configurations in which the complex can be formed with respect to single lattice site: i.e., for a H-vacancy complex it is N_i^{conf}, for an interstitial site z_i^{sites} per host atom.

III. RESULTS OF *AB INITIO* CALCULATIONS

A. Single vacancy

The formalism derived in Sec. II B requires as input formation energies of all relevant defect structures at 0 K. As a first step, we have therefore carried out calculations with an isolated vacancy. In order to determine the formation energy of this defect in the dilute limit without interactions with image defects, the convergence with respect to the supercell size has to be checked.

We therefore consider $2\times2\times2$, $3\times3\times2$, and $4\times4\times4$ supercells, and provide the respective results in Table I. The obtained vacancy formation energies deviate by less than 0.12 eV. In the extrapolated limit of zero-vacancy concentration[50] values of 2.23 eV for the NM and 1.84 eV for the AFMD magnetic structure of fcc Fe are obtained. The results indicate that a $3\times3\times2$ supercell is large enough to yield formation energies accurate to better than 0.1 eV.

An analysis of the atomic structure shows that due to the close packed ordering of fcc Fe the presence of a vacancy has only minor effects on the overall crystal volume. Even for the small $2\times2\times2$ supercell the equilibrium volume is reduced by only 1%. For even smaller vacancy concentrations (corresponding to larger supercells) the volume change becomes negligible. Thus external pressure or internal strain has little effect on the vacancy-formation energy. Even at very high pressures of 10 GPa an increase in only 40 meV is found. We further note that the tetragonal distortion induced by the vacancies in the AFMD crystal structure is negligible.

In the NM structure Fe atoms move toward the center of the vacancy (see Fig. 3), leading to a relative vacancy volume ($\Omega_{\mathrm{f}}^{\mathrm{vac}}/\Omega_0$) equal to 0.66 (for $3\times3\times2$ supercell). The atomic displacements decay almost exponentially with the distance from the defect and are practically restricted to the first four neighbor shells around the vacancy. The situation is qualitatively different for AFMD Fe where a larger vacancy volume of $\Omega_{\mathrm{f}}^{\mathrm{vac}}/\Omega_0=0.75$ is observed. These results are in good agreement with previous LDA calculations of paramagnetic fcc Fe,[37] where the relaxed volume was 0.70. The volume reduction around the vacancy is realized not only by the displacement in the first shell (being in AFMD Fe even higher than in NM Fe) but also by atomic relaxations further away from the vacancy. The resulting elastic field shows a noticeable and oscillating behavior up to the fifth nearest-neighbor shell (see Fig. 3).

A closer inspection of the relaxation shells showed that the larger interaction range of vacancies in the AFMD case is not only caused by strain. Rather, the presence of a vacancy influences the magnetic moments even for atoms that are more than 5 shells away from the defect. Despite the long-range magnetic interaction, the largest effect is on the nearest neighbors and the changes in the magnetic moment show a damped oscillating behavior as function of distance from a vacancy. We note that this effect is strongly anisotropic with the largest oscillation in the (001) plane through a vacancy [plane $f\uparrow$ in Fig. 2(a)].

Introducing a vacancy in the supercell induces a change in the total magnetization by 2.26 μ_{B} and results in a net magnetic moment. Due to atomic and electronic relaxations, the observed change is even larger then a single magnetic moment of 2.05 μ_{B} of an Fe atom in the ideal AFMD crystal.

The magnetic structure of the host system has not only a strong impact on the vacancy formation energy but also on vacancy-vacancy interaction. As can be seen in Table I for the NM case the formation energy decreases with increasing supercell size and thus defect-defect spacing, i.e., vacancies repel each other. In contrast, for the AFMD case vacancies show a net attractive interaction.

The calculated vacancy formation energy in the AFMD is fairly close to the experimental value of 1.7 ± 0.2 eV obtained from positron annihilation.[51] In contrast, a previous DFT-LDA calculation[37] assuming paramagnetic fcc Fe reported a significantly larger formation energy of $E_{\mathrm{f}}^{\mathrm{vac}}=2.65$ eV. We therefore use in the following the AFMD structure to describe vacancy complexes in fcc Fe. As mentioned earlier, complexes with more than one vacancy are energetically highly unfavorable and will not, therefore, be taken into account, i.e., $n_i^{\mathrm{vac}}=1$ or $n_i^{\mathrm{vac}}=0$ (this corresponds to H in interstitial sites) will be assumed in our thermodynamic model.

B. H in interstitial positions

We investigate now the properties of a single interstitial hydrogen atom in an otherwise defect free fcc Fe supercell. The H solution enthalpies for the high-symmetry interstitial sites in bulk fcc Fe, the octahedral site and the two inequivalent tetrahedral sites, are listed in Table I. As can be seen, independent of the magnetic state the OS is energetically always preferred. This observation agrees with previous theoretical investigations[52,53] and neutron spectroscopy experimental studies.[54] The behavior is different for H in bcc Fe for which indirect measurements[1] and several calculations[52,55,56] indicate that the TS is the preferential position.

The hydrogen solution enthalpies as defined in Eq. (4) are virtually identical for NM and AFMD Fe (see Table I). As shown in a previous study, the weak dependence on the magnetic structure is a consequence of a compensation of electronic and volume effects.[53] Nevertheless, the interstitial H atom still shows significant interactions with the Fe magnetic moments.

TABLE I. Reaction enthalpies of solution for H atoms and total formation energies for the *i*th complex at 0 K. Calculations performed in supercells different from $3\times3\times2$ consisting of 72 (71) Fe atoms are marked in the second column. The numbers in the first column correspond to the AFMD structures and label only the structures which are actually used in the thermodynamical evaluation. For these complexes the number of configurations N_i^{conf} is also given.

			NM				AFMD			
i	System (H position)	Variants	N_i^{conf}	$\Omega_{\mathrm{f}}^{\mathrm{def}}/\Omega_0$	ΔH_i (eV)	E_{f} (eV)	N_i^{conf}	$\Omega_{\mathrm{f}}^{\mathrm{def}}/\Omega_0$	ΔH_i (eV)	E_{f} (eV)
0	Vac ($4\times4\times4$)			0.69		2.27		0.63		1.82
	Vac ($3\times3\times2$)		1	0.66		2.30	1	0.75		1.77
	Vac ($2\times2\times2$)			0.65		2.39		0.82		1.76
	1H in Vac ($2\times2\times2$)	1		0.76	−0.31	2.08		0.92	−0.15	1.60
1	1H in Vac	1	6	0.78	−0.28	2.02	4	0.86	−0.16	1.61
2		5					1	0.83	−0.20	1.57
3		6					1	0.87	−0.18	1.59
4	2H in Vac	1,2	3	0.93	−0.31	1.71	2	0.96	−0.19	1.43
5		1,3	12	0.96	−0.23	1.78	4	1.04	−0.17	1.45
6		5,6					1	0.95	−0.20	1.37
7		1,5					4	0.97	−0.17	1.45
8		1,6					4	1.00	−0.17	1.44
9	3H in Vac	1,2,3	12	1.12	−0.19	1.51	4	1.02	−0.16	1.27
10		1,3,5	8	1.19	−0.25	1.53	4	1.18	−0.13	1.31
11		1,2,5					2	1.17	−0.14	1.28
12		1,2,6					2	1.18	−0.13	1.30
13		1,3,6					4	1.21	−0.15	1.29
14		1,5,6					4	1.15	−0.18	1.27
15	4H in Vac	1,2,3,4	3	1.35	−0.23	1.28	1	1.35	−0.15	1.12
16		1,2,3,5	12	1.25	−0.26	1.26	4	1.35	−0.12	1.15
17		1,2,5,6					2	1.36	−0.12	1.16
18		1,3,5,6					4	1.33	−0.16	1.15
19		1,2,3,6					4	1.35	−0.14	1.13
20	5H in Vac	1,2,3,4,5	6	1.50	−0.27	1.02	1	1.53	−0.12	1.00
21		1,3,4,5,6					4	1.51	−0.14	1.01
22		1,2,3,4,6					1	1.54	−0.15	0.97
23	6H in Vac		1	1.62	−0.27	0.75	1	1.70	−0.14	0.86
	7H in Vac			1.88	1.97	2.72		1.95	0.65	1.51
24	H in OS (bulk)		1	0.19	0.04		1	0.25	0.09	
	H in TS (bulk)	TS1		0.30	0.49			0.36	0.34	
		TS2						0.38	0.55	
	H in OS near Vac			0.84	0.07			1.04	0.08	
	H in TS near Vac	TS1		0.96	0.50			1.16	0.34	
		TS2						1.19	0.49	

The importance of the magnetic configuration on the hydrogen reaction enthalpy becomes apparent when comparing the two inequivalent tetrahedral sites that are present in an AFMD calculation [see Fig. 2(b)]. The different ratio of spin-up/spin-down nearest-neighbor atoms (respectively, 4:0 and 2:2) leads to an energy difference of more than 0.2 eV. We consistently find that the preferential positions for an H atom are interstitial configurations where the H is embedded in a large number of like spin atoms (i.e., locally FM-like regions). For H in the OS configuration magnetic relaxations are particularly strong and give rise to a symmetry break: whereas H in NM Fe prefers an on-center configuration, in an AFMD crystal the minimum is off-center. The reason is that the corresponding configuration has five spin-up and one spin-down nearest neighbor for the AFMD case, explaining the shift toward the FM-like configuration, i.e., away from the single spin-down atom [also indicated in Fig. 2(b)].

In an off-center configuration the induced magnetic moment at the H site is small ($-0.01\ \mu_{\mathrm{B}}$). However, it changes the magnetization of the surrounding Fe atoms by up to

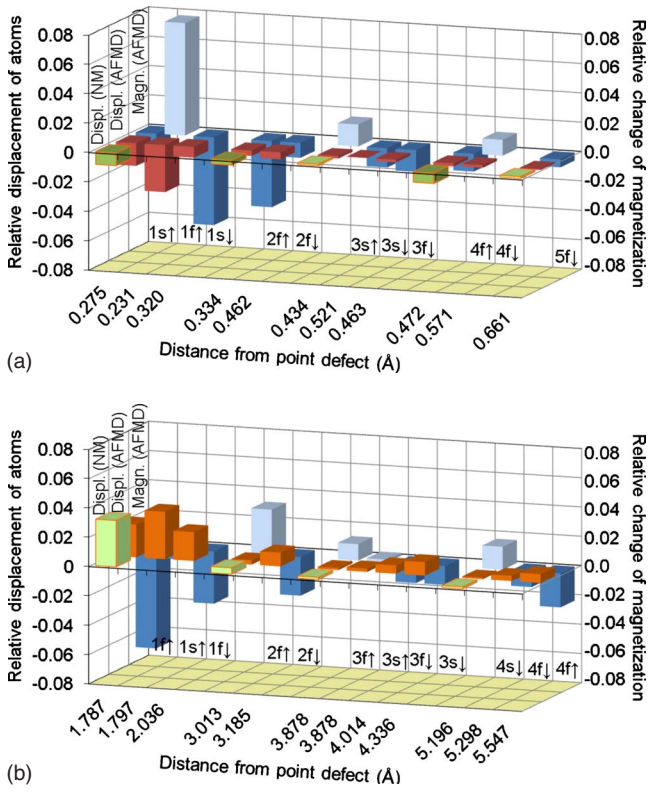

FIG. 3. (Color online) Change in magnetization and displacements of atoms around (a) a vacancy (b) an interstitial H atom in an octahedral site of AFMD Fe at 0 K. Relative changes in the local magnetic moment are determined using the defect and perfect bulk calculation by the following formula: $(\mu_{\mathrm{def}}-\mu_{\mathrm{bulk}})/|\mu_{\mathrm{bulk}}|$. A relative displacement of individual ions is determined by $(\mathbf{r}_{\mathrm{def}}-\mathbf{r}_{\mathrm{bulk}})\cdot\mathbf{r}_{\mathrm{def}}/|\mathbf{r}_{\mathrm{def}}|^2$ using the relaxed position vectors in the defect and the perfect bulk calculation.

$-0.14\ \mu_B$ (see Fig. 3). The biggest change in the local magnetic moments is observed in the $f\uparrow$ plane where an oscillating distance dependence is observed. As a result, the total magnetization of the Fe crystal becomes nonzero resulting in a net increase of $0.52\ \mu_B$ per additional H atom.

In contrast to the long-range changes in the magnetic moments, the decay of the elastic displacements is short range (Fig. 3). Similarly to the vacancy calculations the decay length is shorter in the NM case. We therefore conclude that interstitial hydrogen atoms interact more effectively, i.e., over longer distances by modifying the local magnetic moments than via the elastic field.

The solution enthalpy of an H atom in the bulk and near (but not inside) a vacancy are almost identical. Thus the net strain field around a vacancy is too small to attract/repel H atoms. An H atom diffusing through the lattice will not be attracted by the vacancies and will only be trapped if it accidentally passes a vacancy. We expect thus that the occupation of vacancies by H in fcc Fe will be slow.

For our thermodynamic model we conclude that only one kind of interstitial site (defined by $n_i^{\mathrm{vac}}=0$, $n_i^{\mathrm{H}}=1$, and $N_i^{\mathrm{conf}}=1$) for H needs to be considered. The occupation of the tetrahedral sites for the temperature range considered here (≤ 1800 K) is negligible. Also, a distinction between different OS (dependent on the distance to a vacancy) is not necessary. Finally, the incorporation of several H atoms into the same interstitial site is energetically highly unfavorable and so need not be considered.

C. H-vacancy complexes

Based on the insight gained for the isolated vacancy and interstitial H we now discuss the various hydrogen-vacancy clusters. We first consider the energetics of a single H atom in a vacancy (see Fig. 2). Our results show that the relaxed H atom is neither located in the center of the vacancy, nor in one of the original octahedral sites removed by the vacancy but rather in between. This observation is consistent with previous theoretical findings for H in various bulk metals such as Pd,[6] Be,[57] and Al.[5] More precisely, the displacement of H from the center of a vacancy is equal to $0.35a$ in NM Fe and between $0.39a$ and $0.26c$ in AFMD Fe, depending on the local magnetic configuration. The reaction enthalpies associated with these minima are -0.28 eV for the NM, and -0.16, -0.20, and -0.18 eV for the AFMD case. Therefore, binding to a vacancy for a single H atom is considerably more favorable than occupying a regular bulk interstitial site.

The dependence on the particular magnetic configuration in AFMD Fe is noticeable, though it is comparably small. Consistent with our observations for octahedral sites, H prefers a high coordination of Fe atoms of like spin. As a consequence, H sitting in the plane parallel to the magnetic layers in the AFMD structure [sites 1–4 in Fig. 2(a)] are slightly displaced by 0.10 Å into the magnetic double layer [upward in Fig. 2(a)]. More importantly, the energy for H at the sites 5 and 6 in Fig. 2(a), where the neighboring Fe atoms have the same spin, is smaller by 0.04 and 0.02 eV than for the other sites.

Several additional configurations are possible, if more than one H atom occurs in a vacancy. The energetics of all these configurations is listed in Table I. The energy differences between different H arrangements can be as large as 0.11 eV in NM Fe (for a vacancy occupied with four H atoms) and up to 0.15 eV in the AFMD Fe (three H atoms). These energy differences yield a preference in the atomic arrangement, with the general trend being that the H atoms try to stay apart from each other.

The arrangement of the H atoms in the vacancy influences not only the reaction enthalpies. Also, the occupation number has a significant effect on other crystal quantities that may be accessible to experiment. One example is the tetragonality ($c/a=1.088$ for pure AFMD Fe) which can increase to values up to $c/a=1.100$ for some of the complexes with three or four H atoms. An even larger impact of the specific H arrangement is observed for the net magnetization (Table II). A particularly large effect occurs if H atoms leave the octahedral sites and move into the vacancies. Another macroscopic observable affected by this process is the reduction in the lattice constant, which should be observable by dilatometry.

Independent of the magnetic structure each vacancy can be occupied with up to six atoms, i.e., all six octahedral sites within a vacancy can be occupied with a single H atom. Including more H atoms gives rise to a highly unfavorable

TABLE II. Defect related net magnetic moment and tetragonality in an AFMD $3\times3\times2$ supercell.

Point defect	Net magnetic moment	Tetragonality
Bulk	0	1.088
Only Vac	2.26 μ_B	1.088
1H-Vac	1.77–2.84 μ_B	1.086–1.089
2H-Vac	2.31–3.84 μ_B	1.088–1.095
3H-Vac	3.01–4.34 μ_B	1.088–1.097
4H-Vac	3.66–4.90 μ_B	1.088–1.100
5H-Vac	4.09–5.38 μ_B	1.080–1.088
6H-Vac	4.71 μ_B	1.086
H in OS	0.52 μ_B	1.088

formation energy preventing the formation of such complexes at realistic H chemical potentials. Therefore, we consider in our thermodynamic model hydrogen-vacancy complexes with $n_i^{vac}\leq 6$.

IV. DISCUSSION OF THE THERMODYNAMIC EVALUATION

Based on the DFT computed solution enthalpies we now derive temperature-dependent equilibrium defect concentrations. Although the *ab initio* results show small but not negligible differences between NM and AFMD calculations, we will first discuss the AFMD case and later perform a comparison with other magnetic configurations.

Apart from the case of empty vacancies, the formation energies of all considered defect structures depend, according to Eq. (15), sensitively on the H-chemical potential. Since this dependence is essential for the formation of the various defect complexes, its explicit visualization in Fig. 4 is of central importance for the upcoming discussion. The

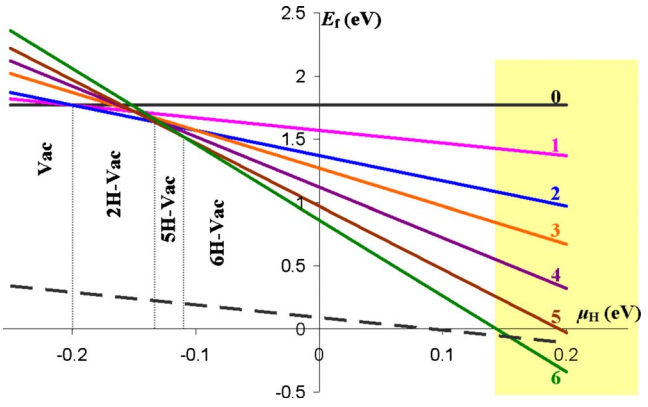

FIG. 4. (Color online) Formation energies of point defects at 0 K for different H chemical potentials. Dashed line—for H in OS and solid lines—for H-vacancy complexes with the number of H shown. The dominant H-vacancy complexes are denoted by labels with vertical direction. The yellow (gray) region for $\mu_H>0.14$ eV shows the thermodynamically forbidden region where the six-H-vacancy formation energy becomes negative, i.e., the crystal is unstable against vacancy formation even at $T=0$ K.

philosophy of the figure is similar to established approaches in the field of charged defects in semiconductors, where formation energies are typically plotted as a function of the electronic Fermi energy.[58] For the present problem, hydrogen takes over the role of the electronic charge in semiconductors, and the number n_H of H atoms involved in the defect determines the slope of the lines in Fig. 4. As a consequence defects with a high H content become, with increasing chemical potential, energetically more and more relevant.

As can be seen for an extreme H-rich condition ($\mu_H>0.14$ eV, marked by the yellow region in Fig. 4) the 6H-vacancy formation energy becomes negative indicating that the Fe crystal will decompose. We will therefore limit our discussion to the thermodynamically allowed range ($\mu_H<0.14$ eV). To relate the H chemical potential to real-world situations we note that at ambient temperature ($T=300$ K) and pressure (1 atm) in rain water it is about −0.33 eV, in distilled water −0.41 eV and in sea water −0.47 eV. However, higher values of μ_H are also easily accessible if H pressures above 1 atm are present. An H pressure of about 30 atm., e.g., is needed to attain a H chemical potential of 0.09 eV at 300 K.

Figure 4 demonstrates on the one hand that in the relevant region for μ_H the energetically most preferable (and thus most abundant) point defects are H atoms in the octahedral interstitial positions. Only if the H chemical potential goes below $\mu_H=-1.77$ eV do empty (i.e., H-free) vacancies become the dominant defect. Thus, as can be seen in Fig. 4, even at extreme H-rich conditions the energetically preferred configuration for H is the bulk OS, i.e., the majority of the H atoms will sit in the OS, and will not form H-vacancy complexes. At first glance this result may appear counterintuitive since the reaction of a vacancy with interstitial H is (for $\mu_H=0$ eV) exothermic. The reason why H is nevertheless predominantly incorporated in bulk interstitials is that the vacancy formation energy itself is highly endothermic, giving rise to the high formation energy of these complexes.

Focusing, on the other hand, on vacancy-related defects, Fig. 4 reveals that not all possible configurations are energetically favorable at $T=0$ K. The formation of a complex with a single H atom, e.g., is always unstable against the occurrence of vacancies that are empty or doubly occupied by hydrogen. In fact, 2H-Vac complexes have the highest concentration at -0.2 eV$<\mu_H<-0.13$ eV, 5H-Vac complexes—at -0.13 eV$<\mu_H<-0.11$ eV and 6H-Vac complexes dominate at higher H chemical potential. The lack of certain occupations is a well-known and established observation in the field of charged semiconductor defects and related to the concept of negative U centers. These observations can be seen as the $T=0$ K results in Fig. 5.

At finite temperatures, however, defect structures which do not have the lowest formation energy can also become macroscopically occupied or even stabilized. In order to analyze this in more detail we have used the thermodynamic model derived in Sec. II B and have calculated the total vacancy concentration in an AFMD Fe crystal. A temperature range from 0 to 1800 K, and typical values of the H chemical potential have been assumed for the visualization in Fig. 5. The boundaries between regions with two different dominant H-vacancy complexes "*a*" and "*b*" are straight lines and de-

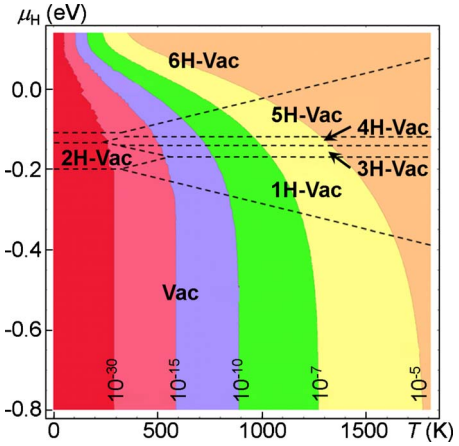

FIG. 5. (Color online) Vacancy concentration as a function of temperature and hydrogen chemical potential for AFMD fcc Fe. The dominant H-vacancy complexes are separated by dashed lines.

termined according to the following equation:

$$\mu_{\mathrm{H}}^{a,b}(T) = \frac{\epsilon_a - \epsilon_b + k_B T \ln R_{ab}}{n_a^{\mathrm{H}} - n_b^{\mathrm{H}}}, \tag{22}$$

where R_{ab} represents the ratio of total configuration numbers for n_b^{H} with respect to n_a^{H} hydrogen atoms.

We observe that some complexes (e.g., with one, three, and four H atoms) which were absent at low temperatures can become the dominating defect type at high temperatures. The stabilization at higher temperatures is related to the higher configurational entropy of H-vacancy complexes with a medium filling. In contrast to the empty and fully occupied complex, for these defects a large number of energetically degenerate configurations exist (see Table I).

The vacancy concentration depends strongly on the absolute value of the external H chemical potential: for low μ_{H} we observe only a small increase but see a rapid increase at high μ_{H}. The total increase in vacancy related defects is dramatic when comparing the H-free case ($\mu_{\mathrm{H}}=-\infty$) with the H-rich case. For high temperatures (e.g., $T=1000$ K) this increase can be as large as 7 orders of magnitude. For low temperatures, where the equilibrium vacancy concentration is very low the increase is even more dramatic. Therefore, the presence of H can lead to the formation of superabundant vacancies.

Due to the large deviation between NM and AFMD in the vacancy formation energy (0.39 eV), a pronounced effect of a change in the magnetic structure is expected for the vacancy concentration in thermodynamic equilibrium. Using the thermodynamic model derived in Sec. II B the equilibrium vacancy concentration has been calculated for both cases and plotted as function of temperature in Fig. 6. As can be seen, the two considered magnetic configurations result in vacancy concentrations ($\mu_{\mathrm{H}}=-\infty$) that differ by up to 9 orders of magnitude at ambient temperature ($T=300$ K). Adding H to the crystal (i.e., increasing the H chemical potential) reduces the discrepancy. However, even at very H-rich conditions (occupying all vacancies with six H atoms) a sizeable difference is still observed. The qualitative trends, however,

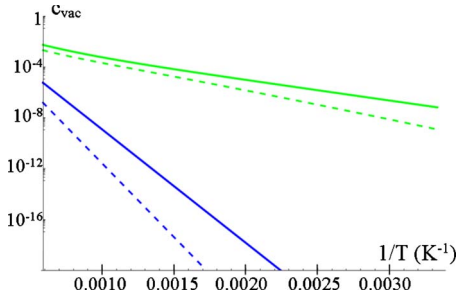

FIG. 6. (Color online) Vacancy concentration obtained from the thermodynamic model derived in Sec. II B assuming a NM (dashed lines) and an AFMD (solid lines) Fe crystal. Blue (dark) lines for $\mu_{\mathrm{H}}=-\infty$ and green lines for $\mu_{\mathrm{H}}=0.09$ eV=const.

are independent of the considered magnetic structures. This independence is expected to remain valid if further magnetic structures such as single-layer AFM, orderings are assumed, since e.g., its vacancy formation energy is close to the value of AFMD state.

Finally, we consider how the presence of vacancies affects the solubility of H in fcc Fe (Fig. 7). As expected from the discussion of Fig. 4 vacancies have little effect on the total H concentration. Only at high temperatures and at extremely H-rich conditions does vacancy formation have a sizeable effect on the H concentration. At low temperatures and low μ_{H}, where practically all H is dissolved in OS, the levels of constant H concentration are described by straight lines yielding direct evidence for Dirac statistics [see Eq. (17)]. All lines start from $\mu_{\mathrm{H}}=0.09$ eV at 0 K, which is the enthalpy of solution for H in OS (see Table I).

V. CONCLUSION

Combining thermodynamic concepts with *ab initio* calculations we were able to study the interaction of H and vacancies in fcc Fe. Our DFT results show that an empty vacancy is a short-range defect in both magnetic and nonmagnetic configurations. The displacement field around the vacancy is

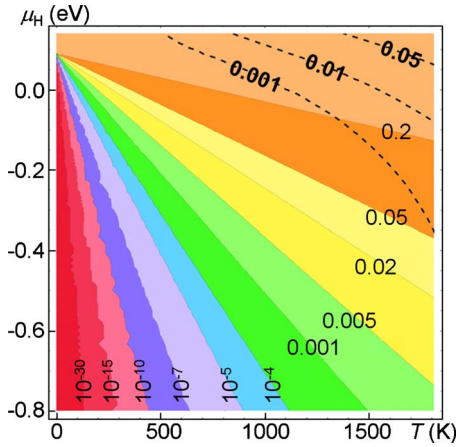

FIG. 7. (Color online) Concentration of hydrogen dissolved in AFMD fcc Fe. Dashed lines—levels of the ratio between H dissolved in vacancies and H dissolved in OS.

more extended in an AFMD as compared to a NM structure. This is due to a twofold effect of removing an Fe atom: it induces a relaxation of the surrounding host atoms toward the vacancy center but also changes the local magnetic moments of neighboring atoms. The latter causes an additional effect due to magnetic interaction. Our spin-polarized calculations show that the presence of a vacancy changes the local magnetization of atoms in a large area (even up to the fifth shell) thus increasing the total magnetization of the system by 2.26 μ_B.

Our results further show that hydrogen in bulk octahedral sites has a similar effect, resulting in a long-range relaxation in the magnetic case and a substantial net-magnetic moment of the system of 0.52 μ_B. Considering an extensive set of H and vacancy-related complexes we find that a single vacancy in a fcc Fe matrix is a highly effective and capacious trap being able to accommodate up to 6 H atoms. Using this DFT data set we derived an analytic thermodynamic model that generalizes previous approaches and that treats the various point defects and complexes in a fully grand canonical ensemble. Applying this model we find that the presence of H can enhance the vacancy concentration by more than seven orders of magnitude resulting in superabundant vacancies. This finding has an important impact on all processes which are related to vacancies, such as, e.g., self-diffusion, creep, phase separation, and should, therefore, be further investigated including the consideration of kinetic effects. Interestingly, despite the huge effect of H on vacancies, the effect of vacancies on the total H concentration is negligible except for at high-temperature and extreme H-rich conditions. Both effects could be explained by using concepts originally developed to describe the electronic charge states as function of the electronic Fermi level. Translating these concepts to the case of varying H occupation in a vacancy, direct and physically transparent insight into the underlying mechanisms could be gained. The suggested concepts are general and can be easily applied to other systems when vacancy-interstitial interactions/complexes are important.

ACKNOWLEDGMENTS

The authors gratefully thank ThyssenKrupp Steel Europe for the cooperation and the funding of the project. Special thanks go to R. Großterlinden, H. Hofmann, T. Pretorius, and I. Thomas for fruitful discussions and comments. We also thank C. Race for careful reading of the manuscript.

*r.nazarov@mpie.de

[1] J. P. Hirth, Metall. Mater. Trans. **11A**, 861 (1980).
[2] N. Eliaz, A. Snachar, B. Tal, and D. Eliezer, Eng. Failure Anal. **9**, 167 (2002).
[3] S. Myers *et al.*, Rev. Mod. Phys. **64**, 559 (1992).
[4] G. Lu, Q. Zhang, N. Kioussis, and E. Kaxiras, Phys. Rev. Lett. **87**, 095501 (2001).
[5] G. Lu and E. Kaxiras, Phys. Rev. Lett. **94**, 155501 (2005).
[6] O. Y. Vekilova, D. I. Bazhanov, S. I. Simak, and I. A. Abrikosov, Phys. Rev. B **80**, 024101 (2009).
[7] Y. Tateyama and T. Ohno, Phys. Rev. B **67**, 174105 (2003).
[8] Y. Fukai, Phys. Scr. **T103**, 11 (2003).
[9] Y. Fukai, J. Alloys Compd. **231**, 35 (1995).
[10] S. Miraglia, D. Fruchart, E. K. Hlil, S. S. M. Tavares, and D. Dos Santos, J. Alloys Compd. **317-318**, 77 (2001).
[11] Y. Fukai and N. Ōkuma, Phys. Rev. Lett. **73**, 1640 (1994).
[12] D. S. dos Santos, S. Miraglia, and D. Fruchart, J. Alloys Compd. **291**, L1 (1999).
[13] Y. Fukai, Y. Ishii, T. Goto, and K. Watanabe, J. Alloys Compd. **313**, 121 (2000).
[14] Y. Fukai and N. Ōkuma, Jpn. J. Appl. Phys., Part 2 **32**, L1256 (1993).
[15] Y. Fukai, Y. Shizuku, and Y. Kurokawa, J. Alloys Compd. **329**, 195 (2001).
[16] K. Nakamura and Y. Fukai, J. Alloys Compd. **231**, 46 (1995).
[17] K. Watanabe, N. Ōkuma, Y. Fukai, Y. Sakamoto, and Y. Hayashi, Scr. Mater. **34**, 551 (1996).
[18] H. K. Birnbaum, C. Buckley, F. Zeides, E. Sirois, P. Rozenak, S. Spooner, and J. S. Lin, J. Alloys Compd. **253-254**, 260 (1997).
[19] Y. Fukai, T. Haraguchi, E. Hayashi, Y. Ishii, Y. Kurokawa, and J. Yanagawa, Defect Diffus. Forum **194-199**, 1063 (2001).
[20] Y. Fukai, K. Mori, and H. Shinomiya, J. Alloys Compd. **348**, 105 (2003).
[21] Y. Fukai and M. Mizutani, Mater. Trans. **43**, 1079 (2002).
[22] P. R. Monasterio, T. T. Lau, S. Yip, and K. J. Van Vliet, Phys. Rev. Lett. **103**, 085501 (2009).
[23] V. Gavriljuk, V. Bugaev, Y. Petrov, A. Tarasenko, and B. Yanchitski, Scr. Mater. **34**, 903 (1996).
[24] A. Khachaturyan, *Theory of Structural Transformations in Solids* (Willey, New York, 1983).
[25] V. N. Bugaev, A. A. Smirnov, and V. A. Tatarenko, Int. J. Hydrogen Energy **13**, 605 (1988).
[26] P. Maroevic and R. McLellan, Acta Mater. **46**, 5593 (1998).
[27] Y. Fukai, Y. Kurokawa, and H. Hiraoka, J. Jpn. Inst. Met. **61**, 663 (1997).
[28] M. Ji, C.-Z. Wang, K. M. Ho, S. Adhikari, and K. R. Hebert, Phys. Rev. B **81**, 024105 (2010).
[29] H. C. Herper, E. Hoffmann, and P. Entel, Phys. Rev. B **60**, 3839 (1999).
[30] I. A. Abrikosov, A. E. Kissavos, F. Liot, B. Alling, S. I. Simak, O. Peil, and A. V. Ruban, Phys. Rev. B **76**, 014434 (2007).
[31] M. Marsman and J. Hafner, Phys. Rev. B **66**, 224409 (2002).
[32] M. Straub, R. Vollmer, and J. Kirschner, Phys. Rev. Lett. **77**, 743 (1996).
[33] D. J. Keavney, D. F. Storm, J. W. Freeland, I. L. Grigorov, and J. C. Walker, Phys. Rev. Lett. **74**, 4531 (1995).
[34] D. Spišák and J. Hafner, Phys. Rev. Lett. **88**, 056101 (2002).
[35] V. Martin, W. Meyer, C. Giovanardi, L. Hammer, K. Heinz, Z. Tian, D. Sander, and J. Kirschner, Phys. Rev. B **76**, 205418 (2007).
[36] D. W. Boukhvalov, Y. N. Gornostyrev, M. I. Katsnelson, and A. I. Lichtenstein, Phys. Rev. Lett. **99**, 247205 (2007).
[37] P. A. Korzhavyi, I. A. Abrikosov, B. Johansson, A. V. Ruban, and H. L. Skriver, Phys. Rev. B **59**, 11693 (1999).

[38] P. Hohenberg and W. Kohn, Phys. Rev. **136**, B864 (1964).
[39] W. Kohn and L. J. Sham, Phys. Rev. **140**, A1133 (1965).
[40] J. P. Perdew, K. Burke, and M. Ernzerhof, Phys. Rev. Lett. **77**, 3865 (1996).
[41] G. Kresse and J. Hafner, Phys. Rev. B **48**, 13115 (1993).
[42] G. Kresse and J. Furthmüller, Phys. Rev. B **54**, 11169 (1996).
[43] G. Kresse and J. Furthmüller, Comput. Mater. Sci. **6**, 15 (1996).
[44] M. Methfessel and A. T. Paxton, Phys. Rev. B **40**, 3616 (1989).
[45] G. Kresse and J. Hafner, Surf. Sci. **459**, 287 (2000).
[46] K. P. Huber and G. Hertzberg, *Molecular Spectra and Molecular Structure IV: Constants of Diatomic Molecules* (Van Norstrand Reinhold, New York, 1979).
[47] G. Henkelman, A. Arnaldsson, and H. Jónsson, Comput. Mater. Sci. **36**, 354 (2006).
[48] E. Sanville, S. Kenny, R. Smith, and G. Henkelman, J. Comput. Chem. **28**, 899 (2007).
[49] L. Ismer, M. S. Park, A. Janotti, and C. G. Van de Walle, Phys. Rev. B **80**, 184110 (2009).
[50] M. I. J. Probert and M. C. Payne, Phys. Rev. B **67**, 075204 (2003).
[51] S. Kim and W. Buyers, J. Phys. F: Met. Phys. **8**, L103 (1978).
[52] C. Elsässer, H. Krimmel, M. Fähnle, S. G. Louie, and C. T. Chan, J. Phys.: Condens. Matter **10**, 5131 (1998).
[53] L. Ismer, T. Hickel, and J. Neugebauer, Phys. Rev. B **81**, 094111 (2010).
[54] S. Danilkin, H. Fuess, H. Wipf, A. Ivanov, V. Gavriljuk, D. Delafosse, and T. Magnin, Europhys. Lett. **63**, 69 (2003).
[55] D. E. Jiang and E. A. Carter, Phys. Rev. B **70**, 064102 (2004).
[56] K. Miwa and A. Fukumoto, Phys. Rev. B **65**, 155114 (2002).
[57] M. G. Ganchenkova, V. A. Borodin, and R. M. Nieminen, Phys. Rev. B **79**, 134101 (2009).
[58] C. G. Van de Walle and J. Neugebauer, Annu. Rev. Mater. Res. **36**, 179 (2006).